Journal of Metals, Materials and Minerals, Vol. 30, No. 4, pp. 19-29, 2020

Quenched and tempered high strength steel: A review

Gadadhar SAHOO*, Krishna Kumar SINGH, and Vinod KUMAR

R & D Center for Iron and Steel, SAIL, Ranchi-834002, Jharkhand, India

***Corresponding author e-mail:** gadadhar@sail.in

Received date:
20 August 2020
Revised date
28 November 2020
Accepted date:
5 December 2020

Keywords:
Martensite;
Tempering;
Hardenability;
Carbides;
Toughness

Abstract

Quenched and tempered steel are broadly classified as low alloy conventional grades with C content of 0.15-0.40% and tool steels with C content as high as 2% alloyed with strong carbide forming elements such as Cr, V, Mo etc. in the range of 1-12%. In both the cases, steels are used in hardened/quenched and tempered or auto tempered condition for improved toughness, strength and wear resistance. The C content and tempering temperature are optimized based on desired application. However, achieving high strength/hardness along with adequate toughness is a challenge. The chemistry design is one of the important parts of developing these grades. The judicious amount of hardenability elements like Mn, Cr, Mo, B etc. are added for achieving required as quenched hardness while excess addition of these elements will not be cost effective. Optimized austenite grain size before quenching is also key to achieve hardenability as well as toughness. All these points have been reviewed systematically in this paper for the first time as there is no such review available covering all aspect of quenched and tempered grade. Unlike text books or any past review articles, this is a systematic review of quenched and tempered steel which will help in designing suitable chemistry and process parameters for producing different grades of quenched and tempered steel in industrial scale.

1. Introduction

Quenched and tempered (Q&T) martensitic steels are widely used in the mining industry, defence (armoured vehicles) and civil construction [1]. In mining industry, the ground engaging tools, transport and earth moving equipments (EMEs) used in various challenging high stress wear conditions, such as mineral haulage and crushing, dredging, demolition of concrete structures, etc. are exposed to abrasive wear and dynamic loads during interaction with hard rocks, which increases the maintenance cost and time associated with replacement or repair [2]. Using improved wear resistant steels for these equipments would significantly benefit the industry. The commercial quenched wear resistant steels are commonly categorized by their Brinell hardness, e.g., as a 400 HB or a 500 HB grade or 550 HB grade steel etc. [3]. Similarly, there are many other Q & T steels used for various applications such as pressure vessel, armoured vehicles and ammunition testing etc. where higher yield strength is required during field operation and hence called as high strength steel. These are Q&T low-alloy steels added with a small amount of B (~20 ppm). The high hardenability of these low alloy martensitic steels is achieved due to the presence of Mn, Cr, Mo and B [4]. The reheating/hardening temperature for austenizing the plate before quenching are optimized to obtain suitable prior austenite grain size, which has direct impact on hardenability as well as toughness [5,6]. In addition to this, hardenability is an issue for thicker plates even through water quenching route, though quenching severity factor of water is higher than that of oil [7]. The important part of product development is to achieve the required mechanical properties like hardness, strength, ductility and Charpy impact energy (CIE). Based on the end application of the Q&T plates, the hardness and toughness varies. Accordingly chemistry and heat treatment parameters are varied for production of these grades.

As hardness primarily depends on C content and hardenability of the particular steel, discussion on hardenability factor consisting of effect of different elements will be also one of the main focuses in this review. In addition to this, the effect of heat treatment parameters such as austenizing temperature, tempering temperature etc. on microstructure and mechanical properties will also be reviewed. Importantly, the recent findings on the effect of grain size on hardenability, the effect of chemical composition on temper embrittlement, the effect of tempering temperature on microstructure etc. have been included in this review, which are not found in any standard text book neither in any review paper on quenched and tempered steel available so far. This review is therefore, systematically aimed at bringing a clear understanding on quenched and tempered grade steel based on which it will be easy in designing alloy chemistry and selecting heat treatment parameters for industrial production economically.

2. Processing and Characterization of Q & T Steel

2.1 Microstructure

The conventional approach to increase wear resistance and penetration resistance of Q&T steels relies on increasing the hardness of the martensitic phase obtained after quenching [8-10]. Martensitic microstructure is obtained through diffusionless shear transformation of austenite, which requires a lattice deformation from FCC austenite to

 DOI: 10.14456/jmmm.2020.47

BCT martensite [11]. The lattice invariant deformation together with the volume expansion from FCC to BCT crystal lattices, creates a high density of imperfections such as dislocation density within martensite crystals. The hardness of martensite mainly depends on the C content in steel composition as lattice distortion increases with increasing C content. Several investigations show that dislocation densities in martensite increase with increased C content [12,13]. Litwlnchuk et al. [8] have found that hardness versus wt% C curve exhibits a maximum value of ~65.5 HRC near 0.9% C in 13 nos. of high purity Fe-C alloy ranging from 0.09 to 1.91% C. They found that the decrease in hardness at C concentrations > 0.9% is the result of a rapid increase in the volume fraction of retained austenite. So, further increase in hardness in steel containing > 0.9% C will only be possible by addition of sufficient ferrite stabilizer and quenching to cryogenic temperature as in the case of high C containing tool steels. Further, the steel weldability, thermal cutting attributes, formability and toughness decrease with increasing C content. In view of this, conventional wear resistance steels are mainly medium carbon (about 0.2-0.4 wt%) martensitic in either quenched and tempered or auto-tempered condition [14]. The C content of the conventional wear resistant steel is practically limited to in the range 0.14-0.40 wt% in steel composition providing corresponding hardness levels in the range of 350-600 HB depending on processing condition [14].

Even though the as-quenched martensite with supersaturated solid solution of C can effectively increase the hardness and strength of wear resistant steels, the martensite structure is rarely used in a non-tempered condition. The martensite in non-tempered condition contains high internal stresses associated with the transformation causing lack in ductility in the material [7,15]. However, the common practice of using these conventional wear resistant steels is either at quenched condition with auto tempering or at low-temperature tempering condition in the range of 150-250°C. This is because, low temperature tempering does not cause much decrease in hardness nor strength as high hardness need to be retained in order to maintain good wear resistance against abrasion [16]. In view of this, the lath martensitic microstructure is retained after tempering of wear resistant grade steel.

2.1.1 Tempering

The as-quenched martensitic microstructure is unstable [11]. A typical light optical micrograph consisting of lath martensitic microstructure of a water quenched steel with 0.21% C, 0.23% Si, 0.92% Mn, 0.48% Cr, 0.24% Ni, 0.0024% B and 0.019% Ti of recent work of this author is shown in Figure 1.

It is well known that mechanical properties of martensitic steel are related to its microstructure, including effects such as carbon evolution, formation of carbide and precipitation of cementite. The high density of dislocations in as-quenched condition creates sites for carbon atom segregation and carbide precipitation within martensite crystals, and a driving force for recovery and recrystallization. The high density of fine martensite crystal interfaces provides also a driving force for boundary rearrangement by recovery or grain growth mechanisms during tempering [11]. As a results of this, the final strength and toughness of the quenched martensitic steels can be adjusted by tempering Therefore, it is important to understand the microstructural evolution of the martensitic steels during tempering to adapt the service requirement.

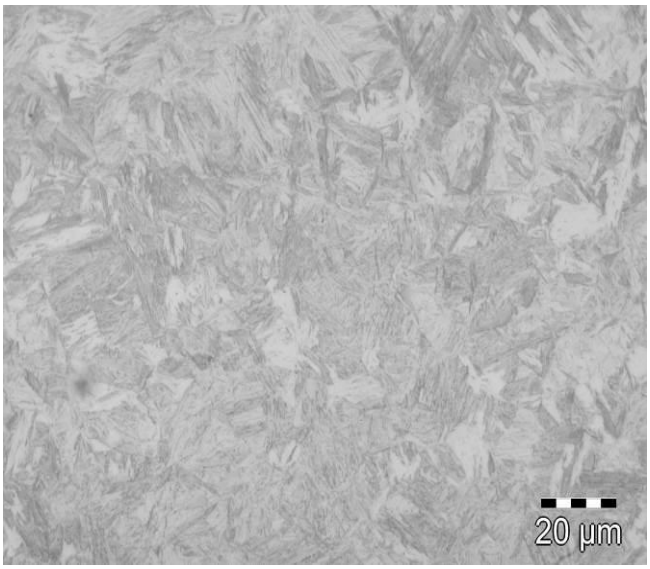

Figure 1. A typical light optical micrograph show lath matrtensitic structure.

2.1.2 Stage of tempering

The classification of the various stages of tempering and the practical effects of tempering of as-quenched martensistic steel was first developed in 1950s [17,18]. The classification system was based on the identification of the carbide phases and the changes in carbide distributions that were formed and evolved during the typically used commercial ranges of temperatures used for tempering. The microstructure change during tempering is generally understood to be composed of four distinct and overlapping stages, i.e. the formation of the transition carbide, the transformation of retained austenite to ferrite and cementite, replacement of transition carbide by cementite and coarsening of cementite along with recrystallization of ferrite [11,19]. Alloy-dependent stage of tempering overlaps the high-temperature tempering range of the fourth stage of tempering [11].

2.1.2.1 First stage of tempering

This stage of tempering is characterized by the precipitation of very fine transition carbides such as of ε-iron carbide or other transition carbides in crystals of martensite at temperature approximately between 100°C and 250°C [19]. The carbide was first identified as having a hexagonal crystal structure with a chemistry of $Fe_{2.4}C$ and was designated epsilon (ε) carbide. An EN48A steel containing 1.45% Si when tempered at 200°C for 1 h shows ε-carbide in cross-hatched morphology while that tempered at 300°C for 1 h shows cementite precipitated in one region of the specimen [20]. Partial loss of tetragonality in the martensite also occurs during first stage of tempering [19]. Excess carbon in the martensite may partition slowly into residual austenite. However, precipitation of ε-carbide of cross-hatched morphology as the first carbide has been reported during first stage of tempering only in steels containing more than about 0.2% C. Further, the attribution of the first stage of tempering is a misnomer, since carbon segregation or precipitation clustering precedes it [21]. The reason of precipitation of ε-carbide is being inhibited in low-alloy steels containing less than 0.2% C is that most of the carbon

in these steels is at dislocation sites. There is little driving force for precipitation as most of these sites have a lower energy than those available in ε-carbide precipitation. On the other hand, when the C content of martensite is increased to 0.4%, the electrical resistivity continuously decreases with time at all temperatures, with no indication of three distinct regions [21]. This is because, at higher C contents not all the carbon can be associated with dislocations and carbide precipitation occurs rapidly even at 150°C.

2.1.2.2 Second stage of tempering

Austenite that is retained as part of almost all martensitic microstructures in carbon steels is unstable below Ac_1, and has to transform during tempering. In this stage of tempering between 200°C and 300°C, retained austenite decomposes into ferrite and carbide along with loss of tetragonality of martensite [11,19]. Retained austenite is present in all groups of carbon steels after quenching to martensite [11]. In general, carbon steels are typically divided into three groups such as low carbon steels with C containing up to 0.20%, medium-carbon steels with C between 0.20 and 0.5% and high carbon with more than 0.5% C as classified by Krauss [22]. Even retained austenite is found to present in low carbon steels containing as little as 0.14% C, which has high M_S temperature [23]. However, the fraction of retained austenite is present in appreciable quantities in low alloy steels when C content exceeds 0.4% [21]. Therefore, the presence of retained austenite during transformation of martensite is considered important only in medium or high carbon steels. Cohen and co-workers [17,18] were able to detect retained austenite by X-ray diffraction measurements as well as dilatometric and specific volume measurements. They had found that the amount of retained austenite is often below 2% in martensitic plain carbon steels with less than 0.5% C, increases to around 6% at 0.8 wt% C and over 30% at 1.25 wt% C.

The transformation of retained austenite as a function of temperature in several medium-carbon steels has been determined by Williamson et al. [24] using Mössbauer spectroscopy. They found that the small amounts of retained austenite are stable until 200°C and the transformation is complete at 300°C. The resulting microstructure shows coarse interlath cementite in martensitic microstructure where an AISI 4340 steel was quenched and tempered at 350°C.

2.1.2.3 Third stage of tempering

Third stage of tempering occurs between 200°C and 350°C with most likely sites of nucleation for cementite are the ε-iron carbide interfaces with the matrix [19]. So, the transition carbides are replaced by intra-lath cementite crystals within martensitic crystals [11]. The resulting microstructure of an AISI 4340 steel after quenched and tempered at 350°C consists of coarse inter-lath plates of cementite [11,23]. As Fe_3C particles grow, the ε-iron carbide particles gradually disappear and martensite now lose their tetragonality and become ferrite. The carbon super saturation has been completely relieved by cementite formation in the parent martensitic matrix, which is now ferrite. However, the microstructure is still referred to as tempered martensite, because it originates from martensitic microstructures, and retains some of the morphological features of martensite [11]. Further, the martensite lath boundaries in low carbon martensites and twin boundaries in the higher carbon martensites are considered as sites for the nucleation of cementite. In the case of Fe-0.38C-0.8Mn-0.5Si-1.7Ni-0.8Cr-0.3Mo wt% quenched steel, rod shaped intra-lath and inter-lath cementite has been reported after tempering at 350°C for 1 h [25]. The initial morphology of cementite in martensite is needle-like when formed either during deliberate tempering or when formed through auto tempering during the quenching of large sections [21]. The formation of these Widmanstatten arrays of Fe_3C rods in both low and high carbon steels also resulted in large hardness decrease [21]. As the tempering temperature is increased this plate-shaped Fe_3C gradually spheroidizes to reduce surface energy.

2.1.2.4 Fourth stage of tempering

The cementite particles undergo a spheroidising and coarsening process in the fourth stage of tempering. The spheroidisation commences between 300°C and 400°C, while coarsening takes place increasingly up to 700°C [19]. As-quenched structure of lath martensite contains low angle dislocation cells and high angle lath boundaries. By tempering at higher temperature, the fine martensitic crystals within the blocks is eliminated, which is attributed to recovery mechanisms associated with the low angle dislocation boundaries, which separates parallel martensite crystals with the same orientation [11]. On increasing tempering temperature, the large angle parallel boundaries rearrange to form equiaxed ferritic grains to minimize grain boundary energy. The microstructure obtained consists of ferrite grains with carbides scattered throughout after long tempering at 700°C [21]. The growth of carbide particles and ferrite grains are the only kinetic processes that continue after completion of recrystallization [21]. Thus, the recovery, recrystallisation and grain growth mechanisms in highly tempered high purity Fe-C alloys and low-alloy steels gives an equilibrium microstructure of spheroidized carbides and equiaxed ferrite grains [11,19]. Further, recrystallization occurs more readily in low carbon steels than in high-carbon steels because the recrystallization process is inhibited by the pinning action of carbides on the boundaries [21].

The microstructure of a 1.20 mm thick 0.24% C, 0.4% Mn, and 0.2% Si containing fully martensitic steel has been studied by Saha et al. [26] using different technique/methods such a s muffle furnace at 500°C for 1 h; and a Gleeble heat treatment (GHT) with a heating rate, temperature, and time of $100°C \cdot s^{-1}$, 495°C, and 1 s, respectively. Two other samples were also tempered using sub-critical HAZ (A_{c1} isotherm line) of diode and fiber laser welded procedure. In the case of DLW sample, the micrographs showed severely tempered structure with highly decomposed martensite with spheroidized carbides at laths boundaries while GHT sample exhibited a comparatively less tempered structure [26]. The furnace heat treatment (FHT) sample tempered in a furnace at 500°C for a 1 h exhibited similar morphologies of spheroidized carbides along with some of the smaller intra-lath carbides. This indicated the presence of a low dislocation density as intra-lath carbides mainly precipitated at dislocation cell structures [26]. The FLW sample showed more dispersedly distributed finer carbides; though with different aspect ratios due to the different heating rate [26]. It is well-known that the maximum number of precipitates is directly proportional to the density of nucleation sites. This maintains an identical size and shape distributions; as a result,

the growth period ceases and the particles directly go from nucleation to coarsening.

Yi *et al*. [27] had studied the effect of tempering at 200-600°C of a 0.18% C, 1.4% Mn, 0.3% Si, 0.2% Cr, 0.2% Mo, 0.02% Ti steel after water quenching from 910°C. The carbide precipitation with nucleation, spherodisation and coarsening kinetics observed on increasing tempering temperature. Some of the carbides begin to spherodise and the carbide amount increases after tempering at 400°C, and precipitates with about 10 nm in size uniformly distribute in the matrix because of the addition of carbide former element such as Ti and Mo. The precipitation of inter-lath carbide at lath boundaries is possible due to the carbide transformation from resolved retained austenite and other impurity segregation between laths. This has probably led to reduction in Charpy impact toughness at this tempering temperature [27].

2.1.3 Auto tempering

The high M_S temperatures of low carbon steels make it possible for the formation of cementite in martensite crystals during quenching, a process referred to as auto-tempering or quench tempering. In the auto tempering process, when steels with M_S temperature above ambient temperature are quenched, there is some brief period in which carbon atoms can redistribute themselves [28]. As the stress fields are created around individual dislocations and cell walls in lath martensite, certain interstitial lattice sites near these defects provide lower energy sites for carbon than the normal interstitial lattice positions. In the case of large section sizes that reduce cooling rates as well as high temperatures below M_S permit the necessary carbon atom diffusion for cementite formation as observed in the case of AISI 4315 steel containing 0.16% C, 0.70% Mn, 0.42% Si, 0.008% P, 0.029% S, 1.84% Ni, 0.78% Cr, and 0.35% Mo [21]. The auto tempering has been also observed in AISI 4130 steel with chemical composition of 0.31% C, 0.57% Mn, 0.85% Cr, 0.15% Ni, 0.18% Mo, 0.28% Si, 0.21% Co, 0.009% S, and 0.008% P when austenitized at 1200°C and quenched in oil due to its high M_S temperature, viz. 350°C [29]. Both cementite and ε-carbide were formed within martensite laths. The ε-carbide formed on {100} planes and the cementite on {110} planes [29]. No lath boundary carbides were observed in the as-quenched specimens.

2.1.4 Temper embrittlement

The loss in toughness in the temperature range 350°C to 550°C of alloy steels previously tempered above 600°C is called tempered embrittlement while tempering as-quenched alloy steels in the range 250°C to 450°C is called tempered martensite embrittlement [30]. The evidence of linking the phenomenon of temper embrittlement to the grain boundary weakening effect of segregated impurities or "tramp" elements (e.g., S, P, Sb, Sn, etc.) has been well established while the mechanism of tempered martensite embrittlement (TME), also known as 350°C still need deeper understanding. Traditionally, embrittlement has been seen when a sudden decrease in ambient temperature Charpy V-notch impact energy and an increase in the Charpy transition temperature [30].

Yi *et al.* [27] had studied the effect of tempering from 200- 600°C of three steels such as steel 1: 0.19% C, 1.5% Mn, 0.3% Si, 0.2% Cr, 0.008% P, 0.02% Ti, steel 2: 0.18% C, 1.5% Mn, 0.3% Si, 0.2% Cr, 0.007% P, 0.2% Mo and 0.2% Ni, and steel 3: 0.18% C, 1.4% Mn, 0.3% Si, 0.2% Cr, 0.015 % P, 0.2% Mo,0.02% Ti. While steel 1 exhibited the highest impact toughness value from 40 to 120 J and Steel 3 has the lowest value from 20 to 110 J due to the high P content. Further, impact toughness increases gradually when the tempering temperature increases from 20°C to 250°C, then the impact toughness sharply drops when tempering at 250-350°C. This drop in toughness is associated with tempered martensite embrittlement. The grain boundary cementite precipitation is one of the reason of embrittlement apart from the other possibility of impurity segregation between laths or blocks [27]. Tempered martensite embrittlement and methods of minimizing it will be further discussed in section 2.3 during discussion of mechanical properties.

2.1.5 Effect of different alloying elements on the formation of iron carbides

The relation between C content (0.12-0.97%) and hardness have been studied after water quenching followed by holding at 196°C [31]. Cryogenic holding was purposefully carried out to minimize retained austenite content. The fall in hardness against at each tempering temperature was also studied. The hardness of as quenched martensite of a particular C content was not changed significantly by adding manganese or other alloying elements [31]. However, the relative decrease in hardness at each tempering temperature is less when other alloying elements are added to Fe-C alloys. Grange *et al.* [31] had studied the effect of alloying elements such as Mn, P, Si, Cr, Mo, V, Ni in the concentration range as per Table 1 on hardness at different tempering temperature in terms of resistance to softening. The resistance to softening is an increase in the hardness (ΔHV) relative to the value on tempering of pure corresponding carbon containing Fe-C alloy at similar tempering temperature.

Table 1. Levels of significant elements in investigated Fe-C alloys and high cleanliness steels [31].

Alloy series (starred element varied)	Levels of element varies (wt%)
Carbon	0.120-0.980
0.5Mn-Carbon	0.080-0.780
0.2C-Manganese	0.350-1.950
0.2C-0.53Mn-Phosphorus	0.002-0.028
0.19C-0.3Mn-Silicon	0.090-0.850
0.18C-0.3Mn-Nickel	0.200-1.550
0.19C-0.3Mn-Chromium	0.100-0.630
0.18C-0.3Mn-Molybdenum	0.060-0.410
0.19C-0.5Mn-Vanadmm	0.020-0.180

2.1.5.1 Effect of manganese

The hardness at different tempering temperature was studied in six high cleanliness pure steels containing 0.2% C and different amounts of manganese in the range 0.35 to 1.97%, which were prepared by vacuum induction melting of electrolytic iron, graphite and pure ferroalloys [31]. It shows that increasing Mn content did not result in a higher hardness substantially when tempered at 204°C while higher hardness was obtained on increasing tempering temperatures to 316°C and above. The increase in hardness on tempering has been attributed to the observed presence of smaller and more numerous carbides [37]. This retards coalescence of carbides, and thus provides a resistance to grain growth in the ferrite matrix along with an apparent lower state of recovery of the martensite (finer packets of ferrite).

2.1.5.2 Effect of chromium

The effect of chromium in the range 0.10 to 0.63% was investigated in 0.19C-0.3Mn steels at different tempering temperature. The increased hardness due to chromium is maximum at 427°C at which the alloy carbides produce maximum strengthening, and then decreases with increasing tempering temperature because the carbides coalesce [31]. Chromium in the percentage range investigated substitutes for some of the iron in cementite, and thus retards coalescence of carbides.

2.1.5.3 Effect of molybdenum

The tempering of the Mo contents in the percentage range investigated as per Table 1 of a 0.15C-0.3Mn steel had no effect at 204°C [31]. However, the increase in hardness with increasing the Mo content was observed as the tempering temperature increased to 538°C. Mo partitions to the carbide phase at elevated temperatures, and thus keeps the carbide particles small and numerous [31]. The increasing trend in hardness starts decreasing with further increase in tempering temperature.

2.1.5.4 Effect of vanadium

As vanadium is a stronger carbide former than chromium or molybdenum, its effect on the hardness of tempered martensite is expected to be more potent. The tempering effect of the V contents in the percentage range as per Table 1 in a 0.19C-0.5Mn steel was investigated with tempering temperature [31]. Though the maximum percentage of vanadium added was only 0.18%, the maximum increase in hardness in specimens tempered at 649°C was considerably greater than that observed with other alloying elements [31]. The large effect of vanadium has been attributed to the formation of an alloy carbide (V_4C or VC), which replaces cementite type carbide at high tempering temperatures and persists as a fine dispersion up to A_1 temperature.

2.1.5.5 Effect of silicon

The effect of Si in the percentage range as per Table 1 in a 0.19C-0.5Mn steel was investigated at different tempering temperature [31]. Si increased the hardness of tempered martensite and it has a much greater effect at 316°C than at other tempering temperatures. This is mainly due to the well-known effect of silicon in inhibiting the conversion of epsilon carbide to cementite. The microstructure of tempered martensite of samples containing 0.09 and 0.86% Si tempered at 649°C showed that the carbides were smaller and the ferrite tended to be divided into smaller lath-like regions (packets) in the 0.86% Si steel [31]. Silicon notably can stabilise the ε-iron carbide to such an extent that it is still present in the microstructure after tempering at 400°C in steels with 1-2 wt% Si, and at even higher temperatures if the silicon is further increased. The evidence suggests that both the nucleation and growth of the carbide is slowed down and that silicon enters into the ε-carbide structure. It is also clear that the transformation of ε-iron carbide to cementite is delayed considerably [32].

Lorimer et al. [33] had studied the effect of Si and tempering temperature on dislocation density, grain size and carbide precipitate size and distribution. They had taken three steels such as Fe-0.44C, Fe-0.43C-0.79Si and Fe-0.44C-1.85Si, hot rolled to 6 mm thick plates and finally cold rolled to 0.6 mm thick strips. After austenizing and quenching, they had tempered the strip at 400, 500, 600 and 700°C for 1 h [33]. The recovery, grain growth and precipitate coarsening had all been retarded due to silicon [33]. Further, the addition of Si retarded the annealing out of dislocations at all temperature investigated by Lorimer et al. [33] and the effect increased with increasing Si content while that of plain carbon steel the dislocation density decreased appreciably even tempering at 400°C. Further, the carbide particles in the plain carbon steel tempered at 400°C for 1h were in the form of rods grown both inside the grains and on the grain boundaries [33]. Higher the tempering temperature, e.g., 500 and 700°C, the particles grown larger and spherodized mostly at grain boundaries and grain boundary triple points respectively [33]. In the case of 0.79% Si steel tempered at 400°C, the carbides are mostly in the lath boundaries. Tempering at 500°C lead to the long string of globular particle at grain boundaries [33]. Tempering of 1.85% Si steel at 400°C resulted in similar distribution but the particle sizes were smaller than low Si steel [33].

2.1.6 Secondary precipitation

Based on hardness changes as a function of tempering temperature of martensite steel, four classes of alloy-dependent tempering behavior have been observed [34]. The class 1 is characteristic of plain carbon and low alloy steels in which hardness decreases continuously. Class 2 represents steels sufficiently alloyed for carbide precipitation but the amount of carbide forming element needed for secondary hardening is not enough. The class 4 may be classified similar to class 2 with a lower carbon concentration leading to a lower as-quenched hardness. The of behavior Class 3 is of typical of highly alloyed tool steels capable of fine alloy carbide precipitation that provides a peak in hardness after tempering at high temperatures [11]. This is termed as secondary hardening. In this case, some strong carbide-forming elements, especially the transition elements such as Cr, Mo, W, V, and Nb are added to steel to slow decrease in hardness or even increase hardness during tempering or service depending on heat treatment and amounts. Several different carbides

might precipitate in the case of steels containing multiple alloying elements [11]. A 2.25% Cr-1.0% Mo containing steel on tempering above 500°C with increasing tempering intensity successively produces carbide dispersions of $Fe_3C + Mo_2C$, $Fe_3C + Mo_2C + Cr_7C_3$, $M_{23}C_6 + Cr_7C_3$, and $M_{23}C_6 + M_6C$, where M indicates combinations of Cr and Mo in a given type of carbide. The formation of alloy carbides as secondary carbides or secondary hardening during tempering in the temperature range 500-600°C is mainly because below this temperature the metallic alloying elements cannot diffuse sufficiently rapidly to allow alloy carbides to nucleate [19]. While metallic elements diffuse substitutionally, C and N move through the iron lattice interstitially for which the diffusivities of C and N are several orders of magnitude greater in iron than those of the metallic alloying elements. As a results of this, higher temperatures are needed for the necessary diffusion of the alloying elements prior to the nucleation and growth of the alloy carbides, which is in the range 500-600°C for most of the carbide-forming elements [19].

More particularly, fine M_2C-type carbides precipitates provides secondary hardening, which are formed by the dissolution of M_3C-type cementite during aging at temperatures near 500°C [35]. While the alloying elements Mo and W form the carbides of M_2C type, and Vanadium forms VC, Cr alone does not form M_2C carbides but form M_7C_3 or $M_{23}C_6$ carbides. Hardening with precipitates of M_7C_3 or $M_{23}C_6$ carbides occurs only by Cr additions greater than about 9% [35]. In the case of lower Cr contents addition of Mo, and/or Co and/or W can contribute to the formation of M_2C carbides dissolved with Cr. Further, C content, required to form M_2C, excess over about 0.25% does not contribute much to the peak hardness due to secondary hardening [35]. The peak hardness of the 0.2% C steel was increased by about 10% but that of 0.4% C steel was decreased by about 5%, as compared to the as quenched hardness for the 4Mo steels [35]. The extent of secondary hardening is eliminated in 2Mo-2.5Cr steel after substitution of Cr for half of the Mo content of the 4Mo steel. The pronounced secondary hardening effect is observed on increasing the Mo content from 2 to 5% in 0.35% C containing steel [35]. Further, either addition of 2% Cr to 2% Mo or substituting Mo partially with 2% Cr in 5% Mo steel resulted in nullifying secondary hardening effect.

2.2 Hardenability

Hardness of quenched plates directly depends on C content as discussed above. However, hardness of hardened steel is governed by hardenability, which is the capacity of steel to be hardened in depth when quenched from austenizing temperature. One of the method to determine hardenability is Grossman's critical diameter (D_c), which is the depth at which 50% martensite and 50% pearlite is formed. In turn, it depends on composition of steel, austenite grain size, the severity of quench and the thickness of steel plate or diameter of the steel bar. While the quenching severity of brine solution is highest and the order of severity is given as brine solution > water > oil > cold gas > air (both in still and agitated condition) depending on thermal conductivity, still the prefer quenchant used is water for the production of the present wear resistant grade as discussed in section 2.1. This is due to the cost effectiveness of the process. The effectiveness of the different quenching media is assessed through quench severity factor (H) [7]. The value of 'H' for quenching in still water is set at 1, as a reference to compare other modes of quenching. In that way, the H factor for oil is 0.25-0.30 and that of brine is 2.0 without agitation [7]. The quench factor increases with agitation. Further, it is felt to express hardenability in such a way, so that the effect of quenching medium can be eliminated. This will be possible by considering standard quenching condition/quenching medium as reference, based on which ideal critical diameter (D_i) will be determined.

The relation between critical diameter (D_c), ideal critical diameter (D_i) and severity of quench determined from thermodynamic known as Grossman's master graph [36,37]. Figure 2 shows the relation between D_c and D_i of steel that can be hardened using a quenching medium with certain quenching severity. From this Figure, when $D_i = 1.2$, $D_c = 1$ for $H = 5$. However, D_c is also increase to 1.2 on increasing H to ∞. Hence, $D_c = D_i$ for $H = \infty$ and $D_c < D_i$ for $H < \infty$.

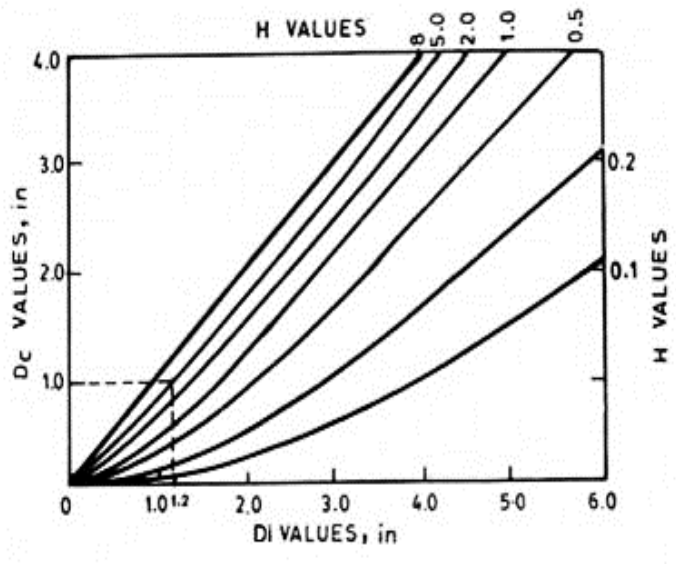

Figure 2. Estimating critical diameter (D_c) in any actual quench of known severity when hardenability of a steel is known in terms of ideal critical diameter (D_i) [36-38] *(with permission from AIST).*

2.2.1 Effect of chemical composition on hardenability

The steel is considered as having a base hardenability due to its C content alone in the case of a "pure steel" of the given C content, without any other elements [38]. The base hardenability in terms of D_i is shown in Figure 3 with respect a particular austenite grain size based on hardening temperature [37]. Furthermore, as the chemical elements also affect hardenability of steel, the base hardenability is multiplied by a multiplying factor for each element present in steel. In view of this, the base hardenability term D_i is now represented with a different term D_{ic} in alloy steel. The resulting ideal critical diameter (Di) of alloy steel will be calculated by multiplying factors of corresponding elements with the base hardenability term (D_{ic}) [38]. The Di is then found from the empirical relationship [7]:

$$D_i = D_{ic} \times 2.21 w_{Mn} \times 1.40 w_{Si} \times 2.13 w_{Cr} \times 3.275 w_{Mo} \times 1.47 w_{Ni} mm \quad (1)$$

Thus, hardenability is of the greatest importance for achieving higher strength in required shapes and sizes and often in very large sections which may be up to a meter or more in diameter in the case of large shafts and rotors. For this, appropriate concentrations of alloying elements need to be added to steel for hardening fully the section of steel under consideration. This is because, most metallic alloying elements slow down the ferrite and pearlite reactions, and thus increase hardenability [7]. However, there is no point in using higher amounts of alloying element, i.e. more than that necessary for full hardening of the required sections as these are much more expensive than iron. The most economical way of increasing the hardenability of plain carbon steel is to increase the Mn content, to about 1.40 wt%, giving a substantial improvement in hardenability [7]. In contrast to this, if two elements are equally effective, a greater hardenability will be obtained by using, for example, 0.5% of each than by using 1.0% of either of them alone [38]. For example, it is observed that an increase from 0 to 0.20% Mn provides a multiplying factor of 1.67, and an increase of Mo from 0% to 0.20% provides a factor of 1.63, an increase of over 60% in each case. However, the factor is raised from 2.65 to 3.35 when Mn increased from 0.50% to 0.70%, an increase of only 26%. Thus the small addition of an element has a much more powerful percentage effect than an equal further addition when its content is already present. Further, in Cr steels (over 0.30% Cr) and Cr-Mo and Cr-V steels, undissolved carbides are likely to be present in the steel as quenched. Hardenability multiplying factors for common alloying elements is shown in Figure 4 [38]. B has a particularly large effect when it's added to fully deoxidized low carbon steel, even in concentrations of the order of 0.001%, if its distribution in steel is properly controlled with the addition of N binding element like Ti. The solubility of boron in steel is reduced when cooled from the hardening temperature. This leads to greater concentration of boron at the grain boundaries as boron carbide $Fe_{23}(BC)_6$ precipitates at the boundary [39]. The presence of boron in solid solution along with coherent boron carbides in the grain boundaries retards the nucleation of ferrite and pearlite and hence increases the hardenability of the steel [39].

In any steel that is quenched, the appearance of ferrite and pearlite corresponds to a large reduction in hardness, as expected from the following empirical equations [40]:

$$HV_{\alpha'} = 127 + 949w_C + 27w_{Si} + 11w_{Mn} + 8w_N + 16w_{Cr} + 21log\ T' \quad (2)$$

$$HV_{\alpha b} = -323 + 185w_C + 330w_{Si} + 153w_{Mn} + 65w_{Ni} + 144w_{Cr} + 191w_{Mo} + (89 + 53w_C - 55w_{Si} - 22w_{Mn} - 10w_{Ni} - 20w_{Cr} - 33w_{Mo}) \times log\ T' \quad (3)$$

$$HV_{\alpha/P} = 42 + 223w_C + 30w_{Mn} + 12.6w_{Ni} + 7w_{Cr} + 19w_{Mo} + (10 - 19w_{Si} + 4w_{Ni} - 8w_{Cr} + 130w_V) \times log\ T' \quad (4)$$

where T′ is the cooling rate in °Ch^{-1}. The equation applies over the range $0.1 < w_C < 0.5$, $w_{Si} < 1$, $w_{Mn} < 2$, $w_{Ni} < 4$, $w_{Cr} < 3$, $w_{Mo} < 1$, $w_V < 0.2$, $(w_{Mn} + w_{Ni} + w_{Cr} + w_{Mo}) < 5$ and w_i represents the wt% of the solute identified in the subscript.

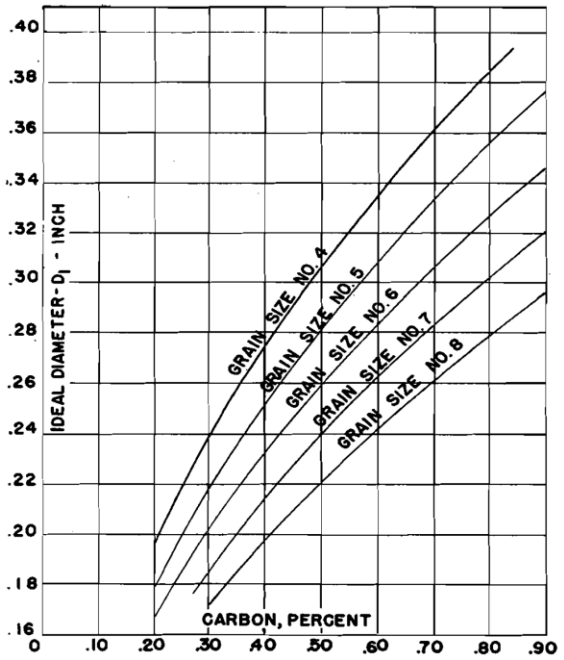

Figure 3. Base hardenability of pure Fe-C alloys, expressed as ideal critical diameter [38] *(with permission from AIST).*

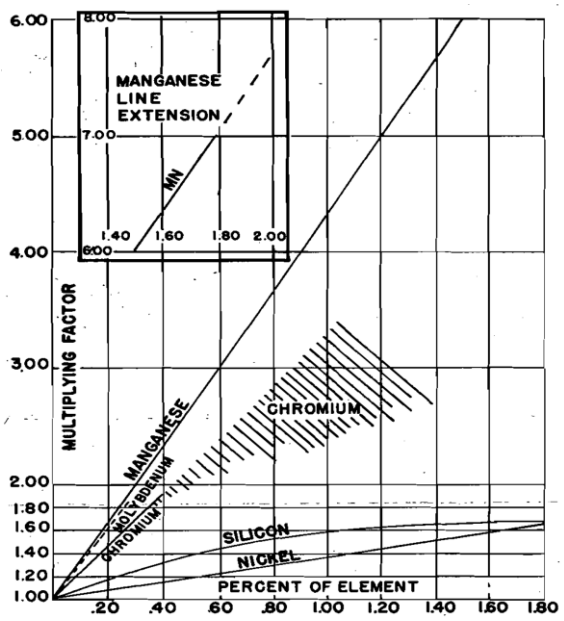

Figure 4. Hardenability multiplying factors for common alloying elements [38] (with permission from AIST).

2.2.2 Effect of austenite grain size on hardenability

Hardenability of steel increases with increasing austenite grain size. This is because, with increase in austenite grain size the grain boundary area decreases. This leads to the decrease in nos. of sites for the nucleation of ferrite and pearlite resulting in slowing down of transformations of these phases. In other words, it facilitates martenistic transformation and hence, the hardenability is increased [7]. The effect of grain size on base hardenability in terms of D_i is shown in

Figure 3. The total hardenability of the steel would then be the product of all the factors, i.e., one for each chemical element present in the steel, and other with a proper correction in multiplying for grain size.

Casero *et al.* [41] have recently found that the grain refinement shifts the martensite start temperature (M_S) to lower values and accelerates the martenistic transformation rate at initial stages during their experimentally studied prior austenite grain size (PAGS) in the range from 6 to 185 μm. When approximately 30% martensite has formed, the transformation rate decreases rapidly for small PAGS, whereas higher rates are maintained in coarse-grained microstructures. The change in martensite formation rate with the grain size depends on the nuclei density and on the austenite strength. As reported in Figure 5, the highest transformation rate is observed for the PAGS of 14 μm at certain under cooling and it decreases with further decreasing grain size. At larger undercooling, microstructures with large PAGSs sustain higher transformation rates than those with small PAGSs. It indicated that the formation of the first martensite fraction takes longer times in microstructures with large PAGSs than in those with small PAGSs. The small PAGSs reportedly sustain higher transformation rates until a martensite fraction of around 0.30 has formed. Clearly, grain refinement increases the density of grain boundary nuclei for martensitic transformation. As reported by Cohen [42] in his earlier study, the initiation of the martensite transformation is controlled by pre-existing nucleation sites like grain boundaries; whereas the progress of the transformation depends on the interplay between pre-existing and auto-catalytically generated defect. The first nucleation event increases interfacial energy (σ), which arises from volume misfit between martensite and austenite, and also increases elastic strain energy (E^{str}), which arises from the shape and volume change that accompanies the phase transformation and is proportional to the volume of the martensite plate/lath. To reduce the energy, the repeated nucleation at the α′/γ front is activated and called as auto-catalytically effect [41].

Cohen [42] observed in a low carbon Fe-Ni alloy that the auto-catalytic factor becomes more important with decreasing PAGS since the forming martensite laths are smaller and more laths have to nucleate in small PAGSs than in large PAGSs to yield the same volume fraction of martensite [43]. However, the combined effect of both an increased density of grain boundary nuclei and a more pronounced autocatalytic factor causes a faster transformation kinetics (higher transformation rate) at initial stages for small grain sizes compared to larger grain sizes and thus, at a given time, microstructures with smaller PAGS form larger fractions of martensite than that of larger PAGS. Casero *et al.*[41] has explained that the formation of the first block/packet of martensite divides the austenite grain into smaller volumes or γ–pockets. As a result of this, subsequent martensite formation occurs in smaller austenite volumes in the same grain with the formation of smaller blocks/packets that efficiently fill the γ–pockets as shown schematically in Figure 6 [41]. In this process, the untransformed austenite is strengthened due to opposite driving force arises from continuous grain refinement, interfacial energy (σ), elastic strain energy (E^{str}) and stored (E^{stored}) energy. The stored energy (E^{stored}) in the parent or product phases (as point defects and dislocations) arises due to plastic deformation caused by the lattice transformation. The austenite becomes stronger because of gradual work hardening during the transformation due to these components. The higher martensite formation rate for small-grained microstructures at initial stages is based on these research finding. The rate slows down after the formation of around a 0.30 martensite fraction due to the plastic strain accumulated in the surrounding γ–pockets appears to exert a higher resistance against the progress of the transformation [43]. Hence, it has been concluded that the strengthening of the austenite phase acts as a main controlling mechanism of the martensite transformation kinetics. For this reason, although the nucleation rate is higher in the case of a small PAGS, the transformation rate decreases rapidly as soon as some austenite volume is consumed and larger under cooling is required to overcome the excess strain energy and proceed with the transformation. In contrast to this, the higher PAGS will have higher transformation rate due to less strain and stored energy. The influence of austenite grain size and strengthening of the austenite phase on the martensitic transformation rate is shown schematically in Figure 7 [41]. In view of this, PAGS can be optimized by controlling austenizing temperature and time before quenching during commercially production of carbon steels.

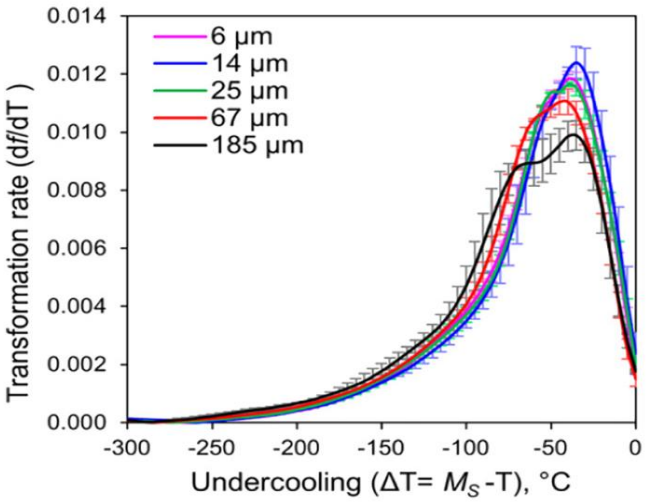

Figure 5. Martensite transformation rate ($df_{\alpha'}/dT$) against undercooling (ΔT). The transformation starts at zero undercooling, which corresponds to the M_S at which the fraction of formed martensite is $f_{\alpha'} = 0.01$ [41].

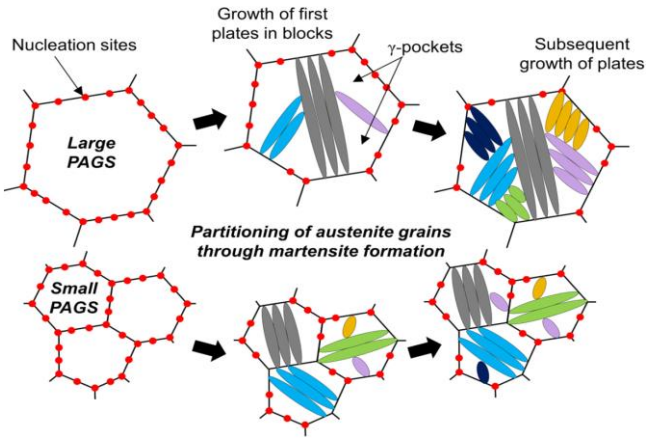

Figure 6. Schematic drawing comparing the progressive partitioning process of austenite grains by martensite plates in large and small grain sizes. Red dots indicate nucleation sites [41].

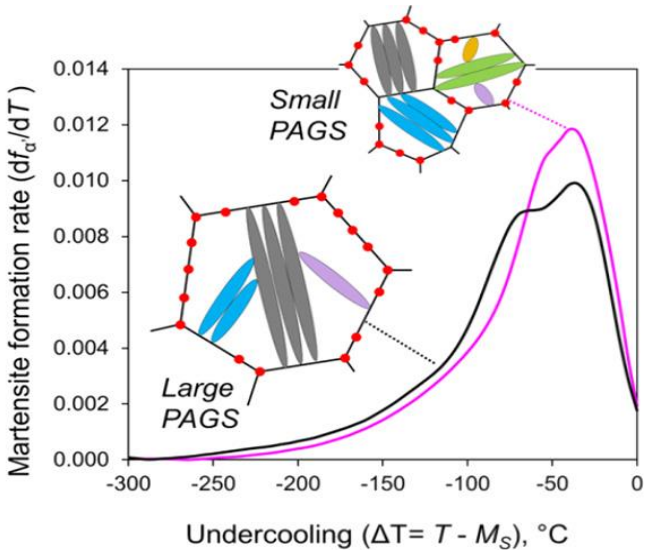

Figure 7. The schematic of the influence of austenite grain size on the martensitic transformation rate through the nuclei density and the strengthening of the austenite phase as the transformation progresses [41].

2.3 Mechanical properties

The effect of C content and tempering temperature on hardness of martensite is already discussed earlier by Grange et al. [31]. The samples were water quenched from austenite region and allowed to hold cryogenically at -196°C as retained austenite converts to martensite on holding at cryogenic temperature though complete elimination of retain austenite is not possible [44]. As discussed, hardness increases with increasing C content and it decreases on increasing tempering temperature for all the range of C containing steel. Further, the effect of different elements on hardness after tempering of low alloy steel at different temperature is already discussed earlier. Yi et al [27] had also studied the effect of tempering temperature at 200-600°C on hardness of martensite, which showed decreasing trend with increasing tempering temperature in all cases. The impact toughness of the three studied steels increases with increasing tempering temperature except at 300-400°C due to tempered martensite embrittlement (TME). The effect of C content on yield strength, tensile strength, ductility and tempering temperature (150, 175 and 200°C) was studied by Saeglitz et al. [44]. They found that the strength parameters decreased and ductility parameters increased continuously with increasing tempering temperature while reverse trend was noticed on increasing C content. The composition also influences TME as discussed below.

Salemi & Abdollah-zadeh [45] had studied mechanical properties of a NiCrMoV steel with 0.34% C, 0.26% Mn, 0.28% Si, 2.53% Ni, 1.29% Cr, 0.57% Mo, 0.15% V, 0.007% S, 0.012% P after austenitized at 870°C for 1 h, followed by oil quenching, and then tempered at temperatures in the range of 200-600°C. The yield strength (YS) and ultimate tensile strength (UTS) decreased on increasing tempering temperature while the reduction in area and elongation increased slightly with the increase of tempering temperature. The room temperature impact energy improved by increasing the tempering temperature with no evidence of TME. As discussed earlier, one of the main mechanisms for TME is the segregation of impurity elements, primarily P and S at the austenite grain boundaries during austenitization and tempering. However, the lack of TME in the steel studied here was attributed to firstly, the combined amount of Mn and Si in this steel (Mn+Si=0.54%) is lower than the minimum amount required for TME to take place, i.e. 0.73 to 1.04 [45]. This is because the higher amounts of Mn and Si enhances the segregation of impurities like P at austenite grain boundaries during austenitization. The other important reason is the relatively high amount of Mo (0.57%) in this steel, which decreases the susceptibility to TME. The interaction of Mo with P can prevent its segregation to grain boundaries, leading to the alleviation of TME. Mo is seen to increase the activation energy for P diffusion and also the binding energy of P in the γ-Fe lattice which could lead to a slower diffusion and a lower concentration of P at the grain boundaries. In contrast to this, TME occurred in all three steels studied by Yi *et al.* [27] where the combined Mn and Si were sufficiently high along with low Mo content (0.2%).

Further, austenite grain size before quenching also influences strength and toughness of Q&T steel. Mani and Udhayakumar [6] had studied a low alloy steel tubes (0.21% C, 0.42% Si, 1.1% Mn, 0.01% P, 0.002% S, 0.2% Cr, 0.02% Al, 0.03% Ti, and 0.0015% B) of outer diameter 25.4 mm, which was induction hardened at two different temperatures (above A_{c3} temperature) 880 and 1080°C and then water quenched. The resulted prior austenite grain size was 20 μm and 100 μm, respectively. While fine lath martensitic structure was observed in the samples induction hardened at 880°C, the coarse lath martensitic structure was observed in the samples induction hardened at 1080°C. Both UTS and YS decreased with increase in tempering temperature. Ductility of the samples improved on increasing tempering temperature. In as quenched condition, the samples induction hardened at 880°C had higher YS and UTS than those induction hardened at 1080°C. Further, energy absorbed of the samples induction hardened at 880°C was higher than that of the samples induction hardened at 1080°C at all tempering temperatures due to lower austenite grain size in the case of former (20 μm). The drop in YS an UTS after tempering was attributed to the recovery of martensitic laths and decrease in quantity of interstitial C atoms in the matrix.

Effect of Si and Ni has been beneficial in improving toughness of steel. These elements refine grains. In addition to this, most importantly these elements produce fine carbides and delay in spherodisation. A 0.86% Si containing steel showed smaller and finer carbides while ferrite tended to be divided into smaller lath-like regions (packets) when tempered at 649°C [37]. The finer carbides and finer lath structure improves toughness.

3. Conclusions

The important points inferred from this review are given below:

- Q &T low and medium carbon steels are used for various applications such as earth moving, construction, pressure vessel, armoured vehicles and ammunition testing etc. The high strength is achieved through quenching while toughness is achieved through tempering process.
- Quenched and tempered grades are either auto tempered or tempered at different temperatures based on the required strength

and toughness. Low C martensite has high M_S temperature and thus, get sufficient time during quenching for auto-tempering.

- Hardness increases on increasing tempering temperature as the concentration of the elements like like Mn, Mo, V, Si etc. increases in the steel, though the increase in hardness is less than the as quenched hardness. The hardness increases upto 350°C tempering in the case of Si while it is 538°C in the case of Mn.
- Uniformly distributed rod shaped carbides are beneficial for strength as well as toughness of plate while tempering between 300-400°C need to be avoided to avoid martensite tempered embrittlement. Mo and V helps in forming M_2C type fine carbides.
- While Mn helps in retaining smaller and more numerous carbides by retarding coalescence of carbides, Si stabilises ε-carbide to such an extent that it is still present in the microstructure after tempering at 400°C.
- The effect of secondary hardening between 500°C and 600°C is observed when strong carbide forming elements like Mo, Co and V are present more than about 1.5% for forming M_2C type fine carbides. In the case of Cr, the minimum quantity is about 9% as Cr forms $M_{23}C_6$ and M_7C_3 type carbides.
- Hardness of martensite will be achieved only if sufficient amount of hardenability elements like Mn and Cr are present while B content is restricted within 20 ppm. The effects of two elements having similar hardenability should be added with 50-50% instead of keeping one element 100% as the effectiveness of hardenability of a particular elements decreases after certain level. Addition of these elements is required, especially for thicker plates to achieve hardenability.
- Effect of hardenability of Cr is minimized after 0.3% due to formation of carbides.
- Hardenability increases with increasing austenite grain size though the initial transformation rate is higher for small austenite grain up to the formation of 0.30 martensite fraction. In contrast to this, toughness of martensite decreased with increasing austenite grain size.

References

[1] K. Valtonen, N. Ojala, O. Haiko, and V. Kuokkala, "Comparison of various high-stress wear conditions and wear performance of martensitic steels," *Wear*, vol. 426-427, pp. 3-13, 2019.

[2] K. Holmberg, and A. Erdemir, "Influence of tribology on global energy consumption, costs and emissions," *Friction*, vol. 5, pp. 263-284, 2017.

[3] N. Ojala, K. Valtonen, V. Heino, M. Kallio, J. Aaltonen, P. Siitonenand, and V. Kuokkala, "Effects of composition and microstructure on the abrasive wear performance of quenched wear resistant steels," *Wear*, vol. 317, pp. 225-232, 2014.

[4] T.G. Digges, C.R. Irish, and N.L. Carwile, "Effect of boron on the hardenability of high-purity alloys and commercial steels," *Boron-Treated Alloys, RPl 938*, vol. 41, pp. 545-574, 1948.

[5] T. Hanamura, S. Torizuka, S. Tamura, S. Enokida, and H. Takechi, "Effect of austenite grain size on transformation behavior, microstructure and mechanical properties of 0.1C–5Mn martensitic steel," *ISIJ International*, vol. 53, pp. 2218-2225, 2013.

[6] E. Mani, and T. Udhayakumar, "Effect of prior austenitic grain size and tempering temperature on the energy absorption characteristics of low alloy quenched and tempered steels," *Materials Science & Engineering A*, vol. 716, pp. 92-98, 2018.

[7] S.H. Bhadeshia, Chapter 8-Heat treatment of steels: Hardenability, steels: Microstructure and properties, 4th edition, Elsevier, 2017, pp.217-236.

[8] A. Litwlnchuk, F.X. Kayser,h. and H. Baker, "The Rockwell C hardness of quenched high-purity Fe-C alloys containing 0.09 to 1.91% C," *Journal of Materials Science*, vol. 11, pp. 1200-1206, 1976.

[9] G.J. Gore, and J.D. Gates, "Effect of hardness on three very different forms of wear," *Wear*, Vol. 203–204, pp. 544-563, 1997.

[10] G. Krauss, Principles of heat treatment of steel, ASM, Metals Park, OH, 1980, pp.52.

[11] G. Krauss, "Chapter 5: Tempering of martensite in carbon steels" *in Phase Transformations in Steels, Diffusionless Transformations, High Strength Steels, Modelling and Advanced Analytical Techniques*, Elsevier, vol. 2, 2012, pp. 126-150.

[12] L-A Norstrom, "On the yield strength of quenched low-carbon lath martensite," *Scandinavian Journal of Metallurgy*, vol.5, pp. 159-165, 1976.

[13] S. Morito, J. Nishikawa, and T. Maki, "Dislocation density within lath martensite in Fe-C and Fe-Ni alloys," *ISIJ International*, vol. 43, pp. 1475-1477, 2003.

[14] A.R. Chintha, "Metallurgical aspects of steels designed to resist abrasion, and impact-abrasion wear," *Materials Science and Technology*, vol. 35, pp. 1133-1148, 2019.

[15] S. Denis, A. Simon, and G. Beck, "Estimation of the effect of stress/phase transformation interaction when calculating internal stress during martensitic quenching of steel," *Transactions ISIJ*, vol. 22, pp. 504-513, 1982.

[16] O. Haiko K.Valtonen. A. Kaijalainen, S. Uusikallio J. Hannula, T. Liimatainen and J. Kömi., "Effect of tempering on the impact-abrasive and abrasive wear resistance of ultra-high strength steels," *Wear*, vol. 440-441, pp. 203098, 2019.

[17] B.S. Lement, B.L. Averbach, and M. Cohen, "Microstructural changes on tempering iron-carbon alloys", *Transactions ASM*, vol. 46, pp. 851-881, 1954.

[18] B.S. Lement, B.L. Averbach, and M. Cohen, "further study of microstructural changes on tempering iron-carbon alloys", *Transactions ASM*, vol. 47, pp. 291-319, 1955.

[19] H. Bhadeshia, and R.Honeycombe, "The Tempering of Martensite," *in Steels: Microstructure and Properties",* (Fourth edition, Elsevier, 2017, pp. 237-270.

[20] J. Gordine, and I. Codd, "The influence of silicon up to 1.5 wt% on the tempering characteristics of a spring steel," *Journal of The Iron and Steel Institute*, vol. 207, pp. 461-467, 1969.

[21] G.R. Speich, and W.C. Leslie, "Tempering of Steel," *Metallurgical Transactions*, vol. 3, pp. 1043-1054, 1972.

[22] G. Krauss, Steels: Processing, structure, and performance, materials park, OH, ASM International, 2005.

[23] S. Okamoto, "Strain rate and temperature effects on deformation behavior and mechanical properties of as-quenched low-carbon martensite," MSc Thesis, (1990) Colorado School of Mines, Golden, CO.

[24] D.L. Williamson, J.P. Schupmann, J.P. Materkowski, and G. Krauss, "Determination of Small Amounts of Austenite and Carbide in Hardened Medium Carbon Steel," *Metallurgical Transactions A*, vol. 10A, pp. 379-382, 1979.

[25] B.C. Kim, S. Lee, D.Y. Lee, and N.J. Kim, "In situ fracture observations on tempered martensite embrittlement in an AISI 4340 steel," *Metallurgical and Materials Transactions A*, vol. 22, pp. 1889-1892, 1991.

[26] D.C. Saha, E. Biro, A.P. Gerlich, and Y. Zhou, Effects of tempering mode on the structural changes of martensite, Materials Science & Engineering A673, 2016, pp. 467-475.

[27] C. Yi, W. Zhao-dong, K. Jian, W. Di, and W. Guo-dong, "Effects of tempering temperature and mo/ni on microstructures and properties of lath martensitic wear-resistant steels," *Journal of Iron and Steel Research International*, vol. 20, pp. 70-75, 2013.

[28] D. Kalish, and M. Cohen, "Structural changes and strengthening in the strain tempering of martensite," *Materials Science and Engineering*, vol. 9, pp. 156-66, 1970.

[29] G.Y. Lai, "On high fracture toughness of coarse-grained AISI 4130 steel," *Materials Science and Engineering*, vol. 19, pp. 153-156, 1975.

[30] R.M. Horn, and R.O. Ritchie, "Mechanisms of Tempered Martensite Embrittlement in Low Alloy Steels," *Metallurgical Transactions A*, Vol. 9A, pp. 1039-1053, 1978.

[31] R.A. Grange, C.R. Hribal, and l.F. Porter, "Hardness of Tempered Martensite in Carbon and Low-Alloy Steels, Metallurgical Transaction," vol. 8A, pp. 1775-1785, 1977.

[32] E. Kozeschnik, B. Sonderegger, I. Holzer, J. Rajek, and H. Cerjak, "Computer simulation of the precipitate evolution during industrial heat treatment of complex alloys," *Materials Science Forum*, vol. 539, pp. 2431-2436, 2007.

[33] G.W. Lorimer, R.M. Hobbs, N. Ridley, G.W. Lorimer, R.M. Hobbs, and N. Ridley, "Effect of silicon on the microstructure of quenched and tempered medium-carbon steels," *Journal of The Iron and Steel Institute*, vol. 210, pp.757-764, 1972.

[34] G. Roberts, G. Krauss, and R. Kennedy, Tool Steels, Materials Park, 5th edn, OH, ASM International, 1998.

[35] H. Kwon, C.M. Kim, K.B. Lee, H.R. Yang, and J.H. Lee, "Effect of alloying additions on secondary hardening behavior of mo-containing steels," *Metallurgical and Materials Transactions A*, vol. 28A, pp. 621-627, 1997.

[36] T.V. Rajam. C.P. Sharma, and A. Sharma, Heat treatment: Principles and techniques, revised edition, New Delhi, 2001.

[37] M.A. Grossman, and E.C. Bain, Principles of heat treatment, 5th edition, ASM, Cleveland, Ohio, USA, 1964.

[38] M.A. Grossmann, "Hardenability calculated from chemical composition, *"American Institute of Mining And Metallurgical Engineers, Technical Publication No. 1437, (Class C Iron and Steel Division No. 299)*, New York Meeting, pp. 1-29, 1942.

[39] M. Maalekian, The effects of alloying elements on steels, 2007.

[40] R. Blondeau, P. Maynier, J. Dollet, and B. Vieillard-Baron, "Estimation of hardness, strength and elastic limit of C- and low-alloy steels from their composition and heat treatment," *Memoires Scientifiques de la Revue de Métallurgie*, vol. 72, pp. 759-769, 1975.

[41] C.C. Casero, J. Sietsma, and M.J. Santofimia, "The role of the austenite grain size in the martensitic transformation in low carbon steels," *Materials & Design*, vol. 167, pp. 107625, 2019.

[42] M. Cohen, "Martensitic nucleation - revisited," *Materials Transactions*, vol. 33, pp. 178-183, 1992.

[43] S. Morito, H. Saito, T. Ogawa, T. Furuhara, and T. Maki, "Effect of austenite grain size on the morphology and crystallography of lath martensite in low carbon steels," *ISIJ International*, vol. 45, pp. 91-94, 2005.

[44] M. Saeglitz and G. Krauss, Deformation, "Fracture, and mechanical properties of low-temperature-tempered martensite in SAE 43xx Steels," *Metallurgical and Materials Transactions A*, vol. 28A, pp.377-387, 1997.

[45] A. Salemi, and A. Abdollah-zadeh, "The effect of tempering temperature on the mechanical properties and fracture morphology of a NiCrMoV steel," *Materials Characterization*, vol. 59, pp. 484-487, 2008.